Biomedical Signal Processing and Control 33 (2017) 335–345

Contents lists available at ScienceDirect

Biomedical Signal Processing and Control

journal homepage: www.elsevier.com/locate/bspc

Novel signal processing method for vital sign monitoring using FMCW radar

Mi He, Yongjian Nian *, Yushun Gong

School of Biomedical Engineering, Third Military Medical University, Chongqing, 400038, China

ARTICLE INFO

Article history:
Received 4 July 2016
Received in revised form 21 October 2016
Accepted 9 December 2016
Available online 30 December 2016

Keywords:
Frequency modulated continuous wave (FMCW) radar
Monitoring
Multi-targets
Vital sign

ABSTRACT

Purpose: To prove that frequency modulated continuous wave (FMCW) radar can be applied for continuous and timely monitoring of vital signs for multi-human targets.
Methods: The chest-wall periodic vibration information resulting from respiration and heartbeat is modulated in the reflected electromagnetic wave of radar from the surface of human bodies or tissue boundaries. The range and vibration information of multi-targets is acquired by a Fourier transform and demodulation processing. To further extract the respiration and heartbeat signals from the mixed vibration phase signal when the respiration signal has several significant harmonics and variant frequencies, a novel recovery and separation method based on a double parameter least mean square (LMS) filter is developed.
Results: The FMCW wide-band radar is capable of multiple vital signal monitoring and subject localization under a low signal to noise ratio (SNR). Compared with the bandpass filtering (BPF) method and wavelet transform (WT) method, the proposed method based on a double parameter LMS filter can obtain more accurate respiration and heartbeat signals.
Conclusions: The FMCW wide-band radar is a reliable, robust, and harmless tool for continuous and timely monitoring of cardiac and respiratory rates for multi-human targets, which has a potential to be applied in wards or home healthcare.

1. Introduction

Respiration and heart rate are important physiological parameters in clinical diagnosis and disease prevention; they directly reflect the physiological state of both respiratory and circulatory systems in human beings. Continuous and timely respiratory and heart rate monitoringin general hospital wards offers important indicators of physiological decline, especially as early as 6–24 h prior to adverse events such as cardiac arrest [1]. Compared with traditional methods, such as pneumotachograph and electrocardiography, noncontact micropower radar has advantages of more convenience for patients and continuous and timely respiratory and heart rate monitoring without additional work load for nurses [2]. The advantages make noncontact micropower radar a favourable option for hospital monitoring, especially for severe burn or infectious disease patients, sudden infant death syndrome monitoring, sleep apnoea monitoring, elderly home healthcare, and psychology studies [3].

In recent decades, three types of micropower radars have been applied in noncontact vital signal monitoring: single or double frequency continuous wave (CW) Doppler radars [4–9], ultra-wide-band (UWB) pulse radars [10–15] and frequency modulated continuous wave (FMCW) radars [16–19]. CW Doppler radars have the advantage of a simple radio structure and low power consumption. However, reflection from other moving objects or people can contaminate echoes from a single vital target using this radar type [20]. UWB pulse radars achieves high spatial resolution but is constrained by pulse width and radar peak signal intensity [17,21]. The FMCW wide-band radar combines the ranging capability of UWB radars with the sensitivity and robustness of CW Doppler radars. This combined advantage is a benefit for micro motion information (because of oscillations in the chest wall [22]) in detecting and monitoring multi-targets located at different ranges [16]. In addition, the FMCW wide-band radar has the potential to have a small size, be light weight, consume low amounts of power and enable real time processing [23]. Thus, the FMCW wide-band radar is more reliable when used in suboptimal environments such as hospital wards and the homecare environment.

Several articles have already presented some theoretical signal processing analysis of signal processing of the FMCW radar [17,24].

* Corresponding author.
E-mail address: yjnian@126.com (Y. Nian).

http://dx.doi.org/10.1016/j.bspc.2016.12.008
1746-8094/

However, some key steps like how to obtain vibration information of multi-targets were not specified or formulated. In the separation algorithm of vital signals, many papers would like to implement only a bandpass filtering(BPF) to extract the respiration and heart beat signals for the FMCW radar [1,16,17]. In fact, respiration signals resulting from periodic chest-wall motion frequently have many harmonics and a variable instantaneous frequency that would interfere with reliable detection of the much weaker heartbeat signal [4,25]. Simply, the BPF method cannot efficiently separate these two signals and is not suitable for short time signal processing [4]. Several more sophisticated separation algorithms have been proposed [4,23,25,26]. The wavelet transform(WT) method was applied to separate respiration and heartbeat signals from a mixed physiological signal [26]. Compared with the BPF method, the wavelet transform method can retain the boundaries and energy of the reconstructed signal for a short duration signal [4,26]. However, reconstructed signals are disturbed when the respiration signal comprises harmonics or the instantaneous frequency of the respiration signal varies severely. Adaptive cancellation of respiration harmonics was implemented to enhance the heartbeat signal by minimizing the mean-square error cost function [25]. However, the heartbeat signal cannot be successfully retained as residual signal power related to the heartbeat signal was minimized in the error cost function. To suppress unnecessary periodic fluctuation components, the projection matrix method was proposed to extract the heart rate [23]. However, it was time consuming to conduct the eigenvalue decomposition of the correlation matrix that typically had large dimensions. The largest eigenvalue corresponds to the component with maximum power that may not be the overall unnecessary fluctuation component, i.e., the respiration signal and its harmonics. The continuous-wavelet filter and ensemble empirical mode decomposition (EEMD) based algorithm was applied for cardiopulmonary signal recovery and separation; this algorithm acquired accurate beat-to-beat intervals in the time domain [4]. However, high accuracy could not be achieved when multiple harmonics exist in the respiration signal because the EEMD method may not completely solve the mode mixing by adding white Gaussian noise for the multiple harmonics case [27].

Unambiguous separation and continuous monitoring of vital signs from subjects is important for the FMCW wide-band radar for hospital monitoring and home healthcare. A framework of multi-target monitoring by the FMCW radar is offered based on basic signal processing and formula deduction of the FMCW radar including vibration information demodulation. To suppress possible harmonics of the respiration signal and interference, this paper proposed a novel recovery and separation method for the heartbeat and respiration signals based on a double parameter least mean square(LMS) filter by simulation.

2. Signal processing

2.1. Basic signal processing

The whole signal processing flowchart of the FMCW wideband monitoring radar is shown in Fig. 1. The transmitted signal is de-ramped with the received signal to obtain the beat signal [28]. For real signals, to obtain the beat signal, a designed low-pass filter (LPF) is needed to suppress the high frequency components in the de-ramping processing [28]; then, the real beat signal is orthogonalized into a complex signal. Next, a Fourier transform is conducted on the complex beat signal to complete the range compression. In practical operation, a fast Fourier transform (FFT) is implemented to obtain the range spectrum. For sidelobe reduction, a Hanning window, which can keep the vibration phase information, is applied to the slow time signal before the FFT. To

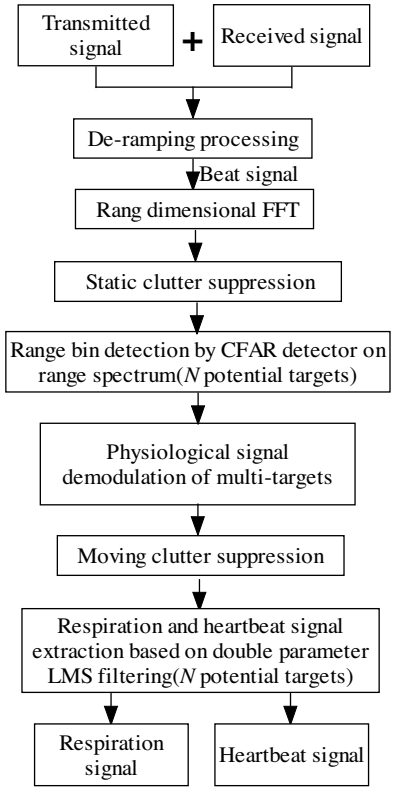

Fig. 1. Overall signal processing flowchart for the FMCW radar monitoring.

detect potential targets, static clutter needs be suppressed. The averaged range spectrum of static environment clutter is usually pre-calculated and saved before the formal radar monitoring work. During subject monitoring, the pre-saved clutter range spectrum is subtracted from the range spectrum including clutter and targets. The range bins n (=1, 2, . . .,N) with potential targets are detected by a constant false alarm(CFAR) detector [29] that is usually used for target detection and identification by conventional radar. The range information of potential targets can be calculated according to range bins. Next, the phase of the n^{th} potential target is demodulated and unwrapped from the FFT result in its corresponding range bin along slow time. After the phase signal is acquired, the direct current (dc) component should be subtracted first for each potential target. To alleviate noise disturbance, a moving average filter is applied to filter the unwrapped phase signal. The frequency peaks in the frequency spectrum of each potential target are computed by a 3-point quadratic interpolation method [25]. Then, the highest peak frequency is evaluated to determine if it falls in the frequency range from 0.1 Hz to 0.5 Hz, which is the typical respiration frequency range for a seated subject at rest. If yes, the range bin of the n^{th} target corresponds to a human target; otherwise, it comprises moving clutter. After this judgement, only $L(\leq N)$ human targets are left. To further suppress moving clutter, a LPF with a cut-off frequency of 4 Hz is used. Then, a double parameter LMS filtering method is developed to extract the respiration signal only with a fundamental frequency and heartbeat signal from the mixed physiological signal of L human targets even when the respiration signal comprises harmonics or the instantaneous frequency of the respiration signal varies. Finally, the range information and extracted respiration and heartbeat signals from each human target are acquired. Some key formulations are presented as following:

Let human targets be indexed by n and characterized by their range R_n^0. The n^{th} human target has the fundamental respiration frequency f_R^n with amplitude $A_{R,1}^n$ and the heartbeat frequency f_H^n with

amplitude A_H^n. The chest-wall quasiperiodic vibration model with M respiration harmonics of the n^{th} human target can be approximated as

$$\Delta R_n(\tau) = A_H^n \cos(2\pi f_H^n \tau + \phi_H^n) + \sum_{m=1}^{M} A_{R,m}^n \cos(2\pi m f_R^n \tau + \phi_{R,m}^n) \quad (1)$$

where τ is the slow time, $A_{R,m}^n$ is the amplitude of the m^{th} respiration harmonic, and $\phi_{R,m}^n$ and ϕ_H^n are the initial phases of the m^{th} respiration harmonic and the heartbeat signal, respectively. The range of the n^{th} human target as a function of the slow time can be written as

$$R_n(\tau) = R_n^0 + \Delta R_n(\tau) \quad (2)$$

If N point targets are illuminated by the coherent FMCW radar, the Fourier transform of the beat signal can be expressed as [18,19]

$$S_b(\xi, \tau) = \sum_{n=1}^{N} B_n \cdot \exp\left(j\frac{4\pi f_c}{c} R_n(\tau)\right) \cdot \operatorname{sinc}\left(T_s\left(\xi - \frac{2k_s R_n(\tau)}{c}\right)\right) \quad (3)$$

where ξ is the fast time frequency, B_n is the backscattering coefficient of the n^{th} target, f_c is the transmitted centre frequency, c is the speed of light, $R_n(\tau)$ is the range of the n^{th} target as a function of the slow time, T_s is the transmitted sweep period, k_s is the chirp modulation rate, and $\operatorname{sinc}(x) = \frac{\sin(\pi x)}{\pi x}$.

If the vibrations of human chest walls along line-of-sight (LOS) are not greater than the range resolution, the scatterers remain in their corresponding range cells during the coherent processing interval (CPI). According to (3), the slow time signal for the range bin in which the n^{th} target is located can be shown as [18,19]

$$s_n(\tau) = B_n \cdot \exp\left(j\frac{4\pi f_c}{c} R_n(\tau)\right) \quad (4)$$

The vibration signal $\Delta R_n(\tau)$ of the n^{th} target can be recovered by unwrapping the demodulated phase signal along a slow time at its corresponding range bin

$$\Delta R_n(\tau) = \frac{c}{4\pi f_c} \cdot \operatorname{unwrap}[s_n] - mean\left(\frac{c}{4\pi f_c} \cdot \operatorname{unwrap}[s_n]\right) \quad (5)$$

2.2. Extraction of respiration and heartbeat signals

Fig. 2 presents the structure to extract respiration signal only at the fundamental frequency and with the heartbeat signal from the mixed physiological signal based on the double parameter LMS filter. This double parameter LMS filter is a well-known generalization to multiple harmonics of the classical LMS filter, which is applied to estimate sinusoidal signals of known frequency [30]. The input mixed physiological signal $s_{mix}^n(i)$ is the discrete vibration signal $\Delta R_n(\tau)$ in slow time. Assume the sampling rate of the vibration signal $\Delta R_n(\tau)$ is f_s. The default value of f_s is the pulse repeated frequency (PRF) of radar. Usually, the vibration signal $\Delta R_n(\tau)$ or $s_{mix}^n(i)$ comprises not only the heartbeat signal but also the respiration signal and its harmonics. The reference signal that is obtained from the mixed signal by moving average filtering and peak detection is called the instantaneous reference signal $\{i_k^n\}$. Because the respiration signal takes up most of the energy in the mixed physiological signal, the instantaneous respiration signal can be approximated as $\{i_k^n\}$.The double parameters $(a_1^n(i), b_1^n(i))$ and $(\boldsymbol{a}^n(i), \boldsymbol{b}^n(i))$ from the LMS filter that are calculated from the reference signal are updated during filtering. The respiration signal calculated only at the fundamental frequency $\hat{s}_{\text{R}}^n(i)$ is adaptively estimated using the model without harmonics. Using the model with harmonics, the respiration signal with its harmonics $\hat{s}_{\text{RC}}^n(i)$ is adaptively computed and subtracted from the input mixed signal to produce heartbeat signal $\hat{s}_{\text{H}}^n(i)$. The detailed steps of the proposed double parameter LMS filtering are as follows.

A. Calculate reference signal

The peaks of the mixed physiological signal after moving average filtering are detected by the peak detection method and are denoted as $\{i_k^n\}$. Because the heartbeat signal is much weaker than the respiration signal, the reference signal can be thought of as the instantaneous respiration signal $\{i_k^n\}$. The interval between consecutive instantaneous measurements corresponds to one oscillatory cycle. Without a loss of generality, the frequency of the respiration signal is assumed to be constant during one cycle but may vary between cycles. For the sampling rate f_s, the instantaneous frequency and phase of the respiration signal of the n^{th} target are calculated as

$$f_k^n = \frac{f_s}{i_{k+1}^n - i_k^n}, \quad i_k^n \le i < i_{k+1}^n \quad (6)$$

$$\phi^n(i) = \frac{2\pi\left(i - i_k^n\right)}{i_{k+1}^n - i_k^n} + 2\pi k, \quad i_k^n \le i < i_{k+1}^n \quad (7)$$

B. Rewrite respiration signal model

The significant harmonic number M of the respiration signal is ensured by checking whether the neighbouring frequency intervals of multiples of the fundamental frequency have peaks on the frequency spectrum of the respiration signal for the n^{th} target. From Eq. (1), the respiration signal and its harmonics of the n^{th} target in discrete signal form can be expressed as

$$\begin{aligned} s_{\text{RC}}^n(i) &= \sum_{m=1}^{M} A_{R,m}^n(i) \cos(m\phi^n(i) + \phi_{R,m}^n(i)) \\ &= \sum_{m=1}^{M} a_m^n(i) \cos(m\phi^n(i)) + b_m^n(i) \sin(m\phi^n(i)) \end{aligned} \quad (8)$$

In Eq. (8), the time-varying amplitude and phase of each harmonic ($A_{R,m}^n(i)$ and $\phi_{R,m}^n(i)$) are equivalent to the amplitude and phase ($a_m^n(i)$ and $b_m^n(i)$) of the in-phase and quadrature components ($\boldsymbol{s}_{\text{I}}^n(i)$ and $\boldsymbol{s}_{\text{Q}}^n(i)$) from the trigonometric function transform.

The in-phase and quadrature components for the M harmonics can be expressed as row vectors

$$\boldsymbol{s}_{\text{I}}^n(i) = \left[\cos\left(\phi^n(i)\right), \cos\left(2\phi^n(i)\right), \cdots, \cos\left(M\phi^n(i)\right)\right] \quad (9)$$

$$\boldsymbol{s}_{\text{Q}}^n(i) = \left[\sin\left(\phi^n(i)\right), \sin\left(2\phi^n(i)\right), \cdots, \sin\left(M\phi^n(i)\right)\right] \quad (10)$$

Arranging the amplitude and phase of the in-phase and quadrature components into column vectors yields

$$\boldsymbol{a}^n(i) = \left[a_1^n(i), a_2^n(i), \cdots, a_M^n(i)\right]^T \quad (11)$$

$$\boldsymbol{b}^n(i) = \left[b_1^n(i), b_2^n(i), \cdots, b_M^n(i)\right]^T \quad (12)$$

where T represents the transpose.

The model of the respiration signal and its harmonics of the n^{th} target can be rewritten as

$$s_{\text{RC}}^n(i) = \boldsymbol{s}_{\text{I}}^n(i)\boldsymbol{a}^n(i) + \boldsymbol{s}_{\text{Q}}^n(i)\boldsymbol{b}^n(i) \quad (13)$$

Specifically, considering the respiration signal with only the fundamental frequency, the in-phase and quadrature components without harmonics is expressed as $s_{\text{I}}^n(i) = \cos(\phi^n(i))$ and $s_{\text{Q}}^n(i) = \sin(\phi^n(i))$. The amplitude and phase of the in-phase and quadrature components are $a_1^n(i)$ and $b_1^n(i)$, respectively. The model of the respiration signal with only the fundamental frequency of the n^{th} target can be rewritten as

$$s_{\text{R}}^n(i) = s_{\text{I}}^n(i)\, a_1^n(i) + s_{\text{Q}}^n(i)\, b_1^n(i) \quad (14)$$

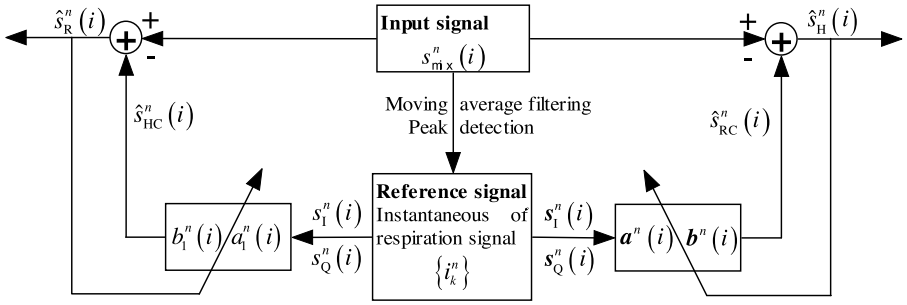

Fig. 2. Diagram of respiration and heartbeat signal extraction method based on double parameter LMS filtering.

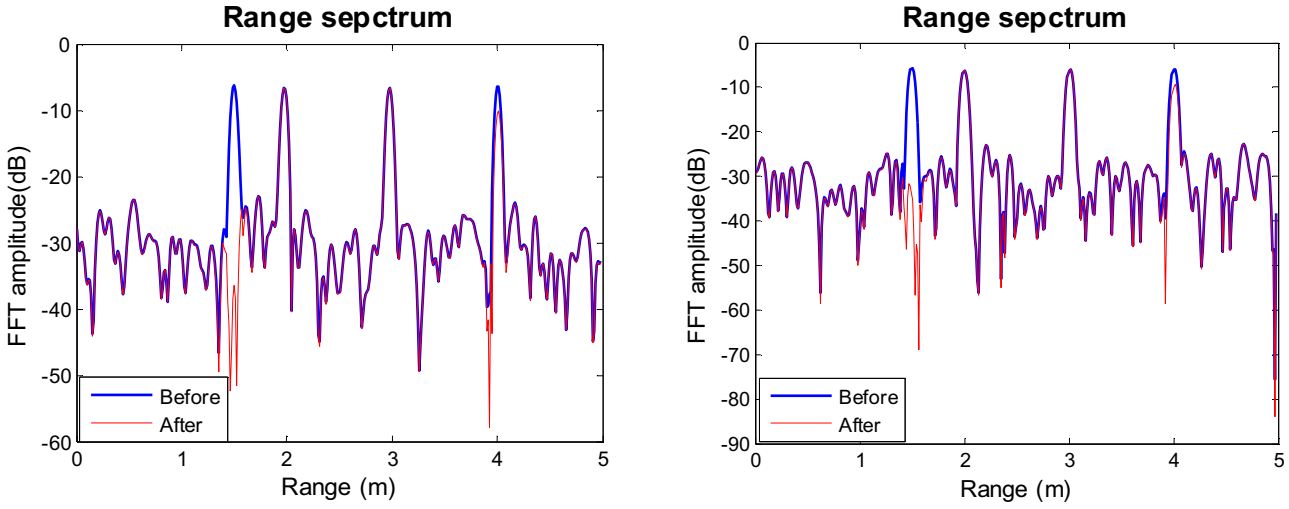

(a) t=0 s (b) t=10 s

Fig. 3. Range spectrums before (coarse line) and after (thin line) clutter suppression at the initial time and at 10 s (SNR = 0 dB, Hanning Window).

C. Assign variant step size

The adaptive filtering step size is assigned to decrease with the harmonic number. The step size for the m^{th} harmonic is

$$\mu_m^n = \frac{1}{m}\mu_0, \quad m = 1, 2, \cdots, M \tag{15}$$

where μ_0 is the initial step size. All step sizes are grouped in a diagonal matrix as follows

$$\boldsymbol{U}^n = \text{diag}(\mu_1^n, \mu_2^n, \cdots, \mu_M^n) \tag{16}$$

D. Estimate respiration and heartbeat signals

The initial value of the double parameters of the LMS filter is set to zero. The respiration signal with only the fundamental frequency is adaptively calculated as

$$\hat{s}_{\text{R}}^n(i) = s_{\text{I}}^n(i)\,a_1^n(i) + s_{\text{Q}}^n(i)\,b_1^n(i) \tag{17}$$

The rest signal, including harmonics and heartbeat signal, is estimated by

$$\hat{s}_{\text{HC}}^n(i) = s_{mix}^n(i) - \hat{s}_{\text{R}}^n(i) \tag{18}$$

The respiration signal and its harmonics $\hat{s}_{\text{RC}}^n(i)$ is adaptively calculated as

$$\hat{s}_{\text{RC}}^n(i) = \boldsymbol{s}_{\text{I}}^n(i)\,\boldsymbol{a}^n(i) + \boldsymbol{s}_{\text{Q}}^n(i)\,\boldsymbol{b}^n(i) \tag{19}$$

The estimated heartbeat signal is computed as

$$\hat{s}_{\text{H}}^n(i) = s_{mix}^n(i) - \hat{s}_{\text{RC}}^n(i) \tag{20}$$

The updated equations of the LMS filter coefficients are

$$a_1^n(i+1) = a_1^n(i) + 2\hat{s}_{\text{HC}}^n(i)\,\mu_0 s_{\text{I}}^n(i) \tag{21}$$

$$b_1^n(i+1) = b_1^n(i) + 2\hat{s}_{\text{HC}}^n(i)\,\mu_0 s_{\text{Q}}^n(i) \tag{22}$$

$$\boldsymbol{a}^n(i+1) = \boldsymbol{a}^n(i) + 2\hat{s}_{\text{H}}^n(i)\,\boldsymbol{U}^n\left(\boldsymbol{s}_{\text{I}}^n(i)\right)^T \tag{23}$$

$$\boldsymbol{b}^n(i+1) = \boldsymbol{b}^n(i) + 2\hat{s}_{\text{H}}^n(i)\,\boldsymbol{U}^n\left(\boldsymbol{s}_{\text{Q}}^n(i)\right)^T \tag{24}$$

If the initial step size is properly selected, the respiration and heartbeat signals can quickly converge and can maintain a smaller steady-state offset the next time with the double parameter LMS filtering [30]. The respiration and heartbeat signals are dynamically estimated with accurate frequency components in real time.

The LMS filter is equivalent to the cascade of M notch filters that are centred in the harmonics of the fundamental frequency. The 3 dB bandwidth of each notch filter is $\frac{\mu_0 f_s}{M\pi}$ [30]. Thus, if the frequency difference between some harmonic of the respiration signal and the heartbeat signal is smaller than $\frac{\mu_0 f_s}{M\pi}$, the amplitude of the heartbeat signal obtained by our method will attenuate larger than 3 dB. However, all the frequency components of the heartbeat signal are maintained and will not affect the heart rate variability analysis. Otherwise, if the frequency difference between some harmonic of the respiration signal and the heartbeat signal is much larger than $\frac{\mu_0 f_s}{M\pi}$, the amplitude of the heartbeat signal acquired by our method will not be severely suppressed.

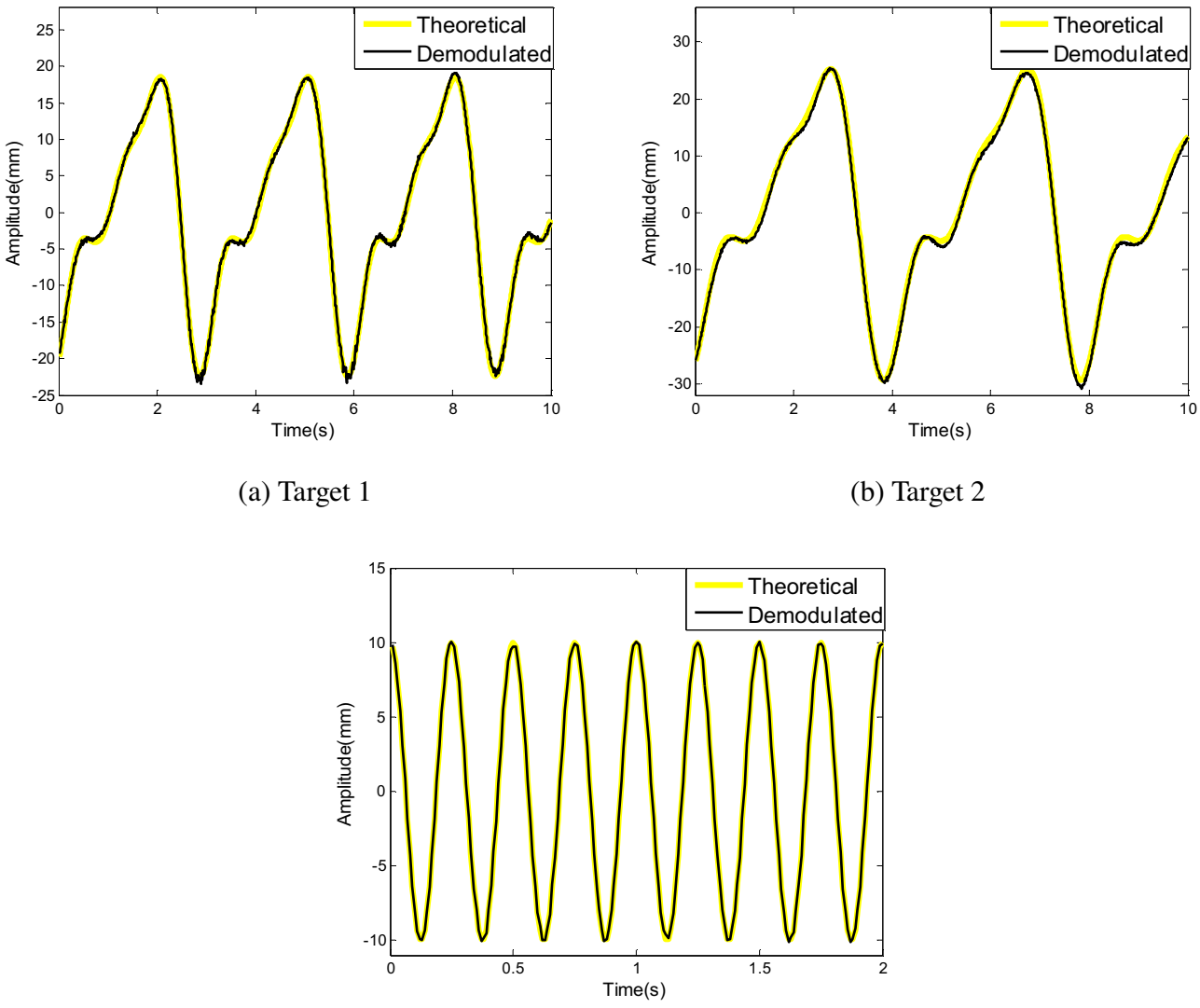

Fig. 4. Demodulated vibration signals of three targets when SNR is 0 dB. The coarser line corresponds to a theoretical value without noise, and the thin line corresponds to the demodulated vibration signal with noise.

Table 1
Parameters of the FMCW monitoring radar.

Parameter	Value	Parameter	Value
Centre frequency	10 GHz	Sampling frequency along fast time	0.67 MHz
Bandwidth	4 GHz	Sampling frequency along slow time	100 Hz
Sweeping period	2 ms	FFT number in the range spectrum	1332
Maximum range	5 m	Range resolution	3.75 cm

3. Simulation and results

The parameters of the FMCW monitoring radar in our simulation are listed in Table 1. The sampling frequency in the fast time is decided by the maximum range [28]. We assume two human targets face radar at distances of 2.0 m and 3.0 m, respectively. For target 1, the fundamental frequency of the respiration signal is 20 breaths per minute (bpm) with an amplitude of 1.5 cm and two harmonics; the frequency of the heartbeat signal is 75 beats per minute (bpm) with an amplitude of 0.5 mm. For target 2, the fundamental frequency of the respiration signal is 15 bpm with an amplitude of 2 cm and two harmonics; the frequency of the heartbeat signal is 65 bpm with an amplitude of 0.6 mm. Assume that static clutter is 1.5 m from the radar and vibrating clutter, with a frequency of 4 Hz and an amplitude of 10 mm, is 4 m from the radar. The observation time of the physiological signal is 100 s. For convenience, let all targets and clutter have the same backscattering coefficients. Without a loss of generality, the signal to noise ratio of the radar receiver is set to 0 dB in the following simulation except when specifically noted.

Fig. 3 shows the range spectrums before and after clutter suppression at the initial time and 10 s, respectively. After clutter suppression, the static clutter at a distance of 1.5 m was perfectly removed by amplitude subtraction of the pre-saved average clutter range spectrum. However, the moving clutter at 4 m cannot be suppressed in this way. The range bins corresponding to the potential targets at 2 m, 3 m and 4 m are detected by a CFAR detector from the range spectrum without static clutter. The FFT phase signal results at corresponding range bins along a slow time are demodulated and unwrapped to obtain the vibration signals, as shown in Fig. 4. From the comparison results, we can see that the demodulated vibration signals have good agreement with the theoretical values. Furthermore, the frequency spectrums of demodulated vibration signals of

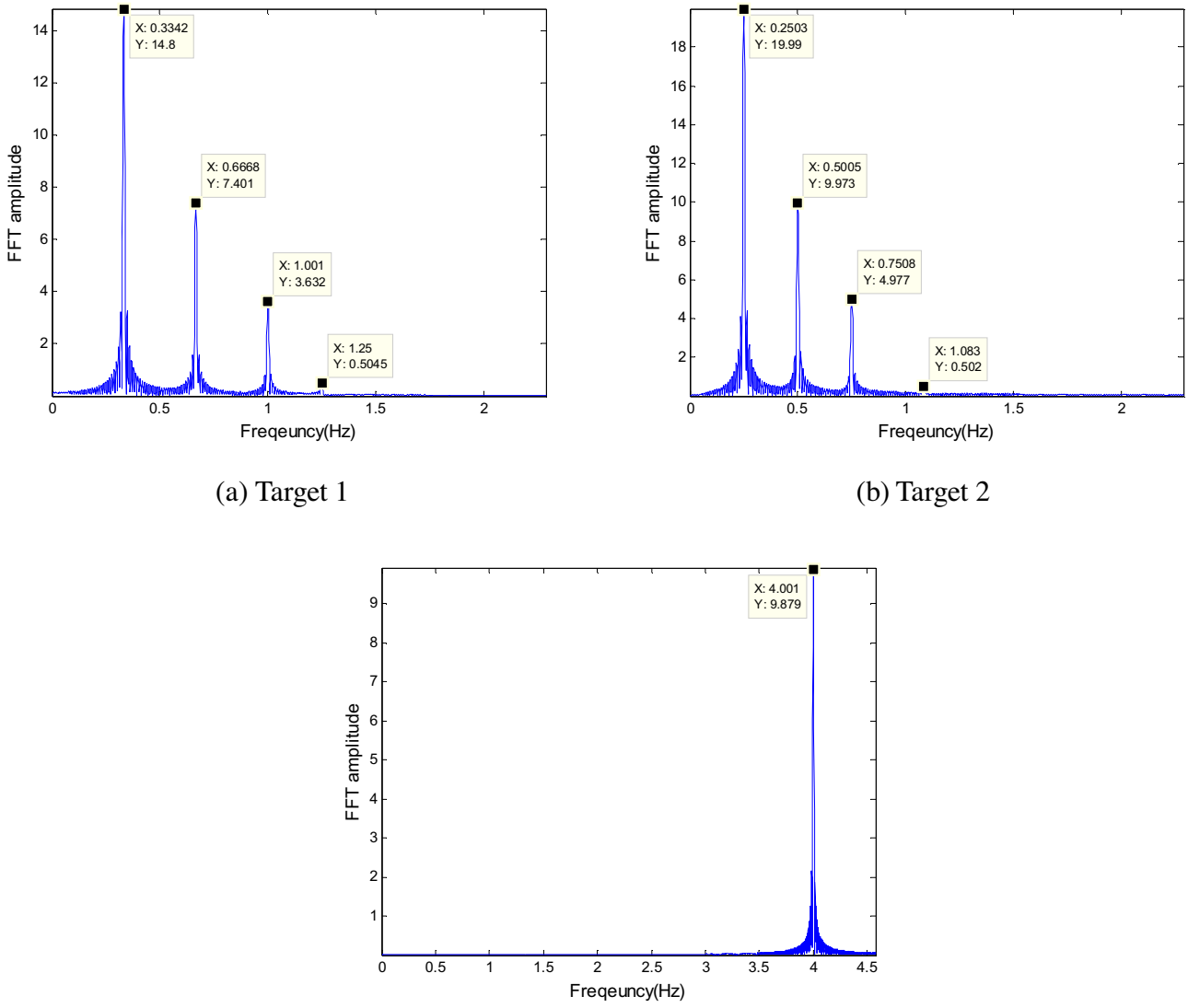

Fig. 5. Frequency spectrums of demodulated vibration signals of three targets (SNR = 0 dB, without windowing).

the three targets are presented in Fig. 5. Taking Fig. 5(a) as an example, the highest peak corresponds to the fundamental frequency of the respiration signal. The next two highest peaks correspond to the frequency of respiration signal harmonics. The lowest peak corresponds to the frequency of the heartbeat signal. From the frequency peak values of potential targets and the decision rule, we can judge that targets 1 and 2 are human targets and target 3 is clutter. The frequency peak values in Fig. 5 are consistent with the respiration and heartbeat frequencies in targets 1 and 2 as well as the vibration frequency of clutter at 4 m, which shows that the demodulated vibration signal agrees with the theoretical signal.

To prove the separation efficiency of respiration and heartbeat signals by our proposed methods, the BPF method and WT method are implemented for simultaneous comparison. A BPF with cut-off frequencies 0.03 Hz and 0.5 Hz [25] is applied for the extraction of respiration signals. Additionally, a BPF with cut-off frequencies of 0.6 Hz and 4 Hz [17] is applied for the extraction of heartbeat signals. Because the sampling frequency of a physiological signal is 100 Hz, the 7-level approximation coefficients of the WT are used to reconstruct the respiration signal, and the detailed coefficients at level 6 of the WT are used to reconstruct the heartbeat signal [26]. All of the extracted signals are compared with the theoretical signal in the time domain. Figs. 6 and 7 show the extracted respiration signals and heartbeat signals produced from three methods of two targets compared with the theoretical respiration signal calculated with only the fundamental frequency. From the results, we can see that the extracted respiration signal and especially the heartbeat signal from our proposed method are more consistent with the theoretical value than the extracted signals from the BPF method and the WT method. Furthermore, the frequency peak values in the frequency spectrum of extracted respiration and heartbeat signals from our proposed methods are presented in Fig. 8. Fig. 8(a) shows that most of the harmonics of the extracted respiration signals of two targets are suppressed compared with the results in Fig. 5(a) and (b). From Fig. 8, we can see that the frequencies of the extracted respiration and heartbeat signals of the two targets can be precisely estimated.

The performance of our proposed method is also tested when the respiration signal frequency varies slowly. For convenience, only one target at 2 m is considered in the following simulation. Fig. 9 presents the physiological signal in the time domain and frequency domain with a fundamental respiration rate varying from

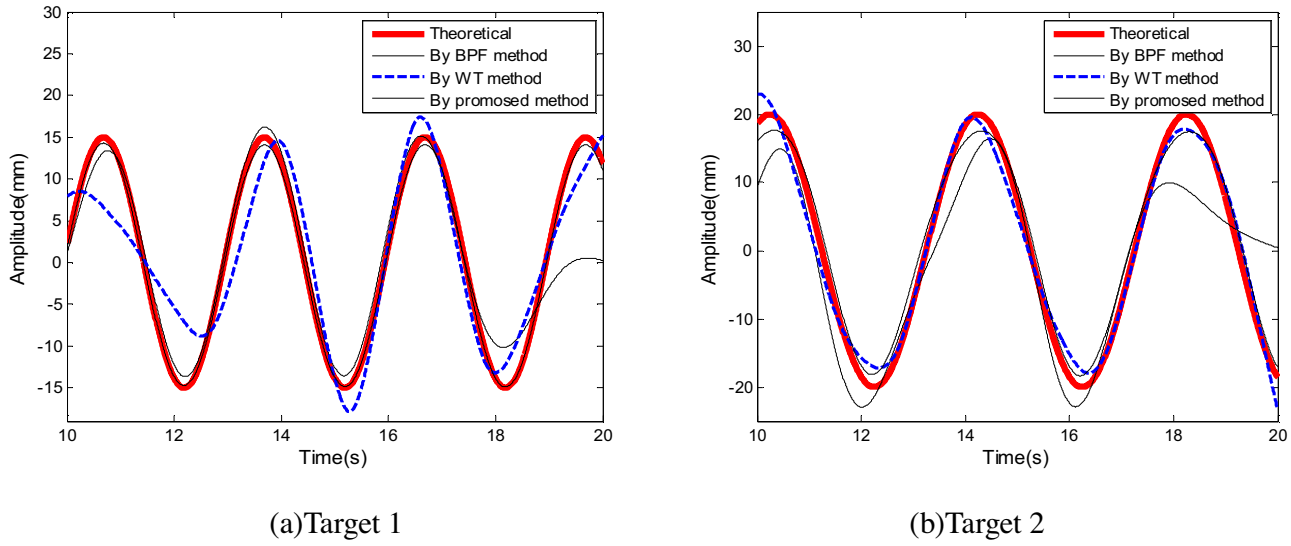

Fig. 6. Extracted respiration signals produced from three methods of two targets compared with the theoretical respiration signal with only the fundamental frequency (from 10 s to 20 s).

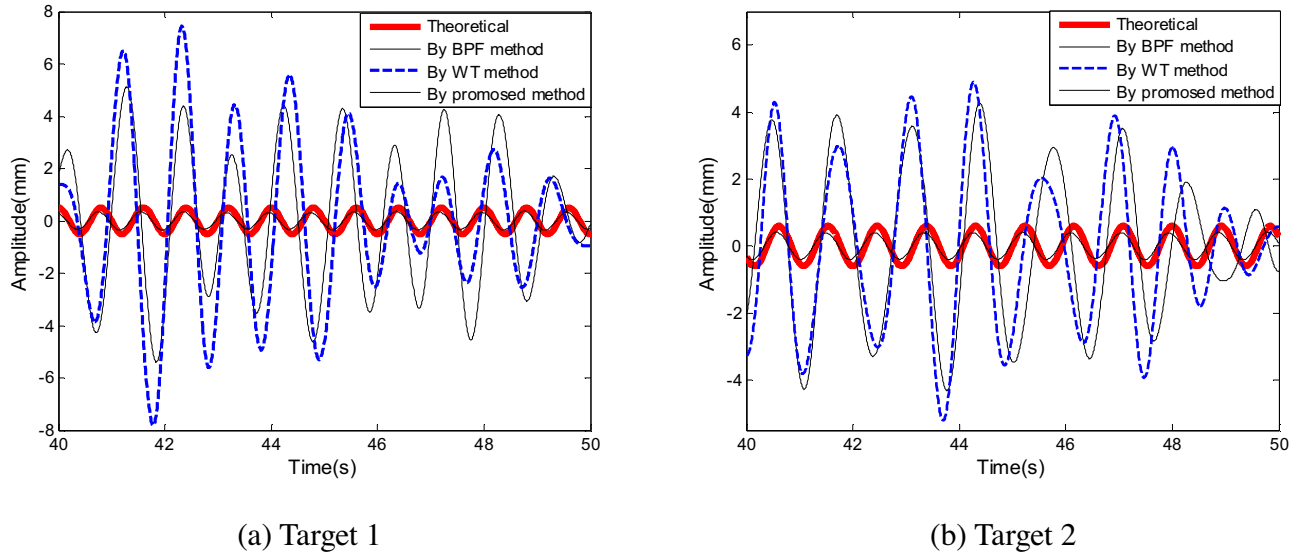

Fig. 7. Extracted heartbeat signals of two targets displayed from the three methods compared with the theoretical heartbeat signals (from 40 s to 50 s).

14 bpm to 20 bpm over 100 s and a fixed heart rate of 75 bpm. The physiological signal comprises the heartbeat and respiration signals with two harmonics. Fig. 9(b) shows that the frequency spectrum of the respiration signal at the fundamental and harmonic frequencies is spread along the frequency axis. The estimated heartbeat signal results are presented in Fig. 10. Fig. 10(a) shows the extracted heartbeat signal compared with the theoretical heartbeat signal in the time domain, which indicates that the estimated heart signal can quickly converge (shorter than 5 s) and maintain a smaller steady-state offset the next time. Fig. 10(b) is the zoomed in picture of Fig. 10(a). Fig. 10(c) gives the frequency spectrum of the extracted heartbeat signal, indicating that the frequency of the heartbeat signal can be precisely estimated even with a varying respiration rate.

Furthermore, frequencies and amplitudes of the extracted heartbeat signals are observed when the heart rate varies from 61 bpm to 80 bpm with a step of 1 bpm and the fundamental respiration rate fixed to 20 bpm with two harmonics. Fig. 11(a) and (b) present the amplitudes and frequencies of the peaks on the frequency spectrums of extracted heartbeat signals, respectively. The results indicate that the amplitude of extracted heartbeat signal increases with heart rate and stays relatively stable when the heart rate is greater than 70 bpm. From Fig. 11(b), the frequencies of extracted heartbeat signals are precisely consistent with the theoretical values; the frequency at 61 bpm can also be precisely estimated because it is close to the frequency of the third harmonic of the respiration signal(i.e., 60 bpm).

Noise of radar RF will affect the frequency estimation performance of vital signs. Fig. 12 shows the mean square error(MSE) changes with the SNR by averaging over 1000 independent Monte Carlo runs. As the frequencies of heartbeat and respiration signals are our concern, the MSE is defined as

$$\mathrm{MSE} = \frac{1}{P}\sum_{p=1}^{P}\left(\hat{f}_p - f_p\right)^2 \tag{25}$$

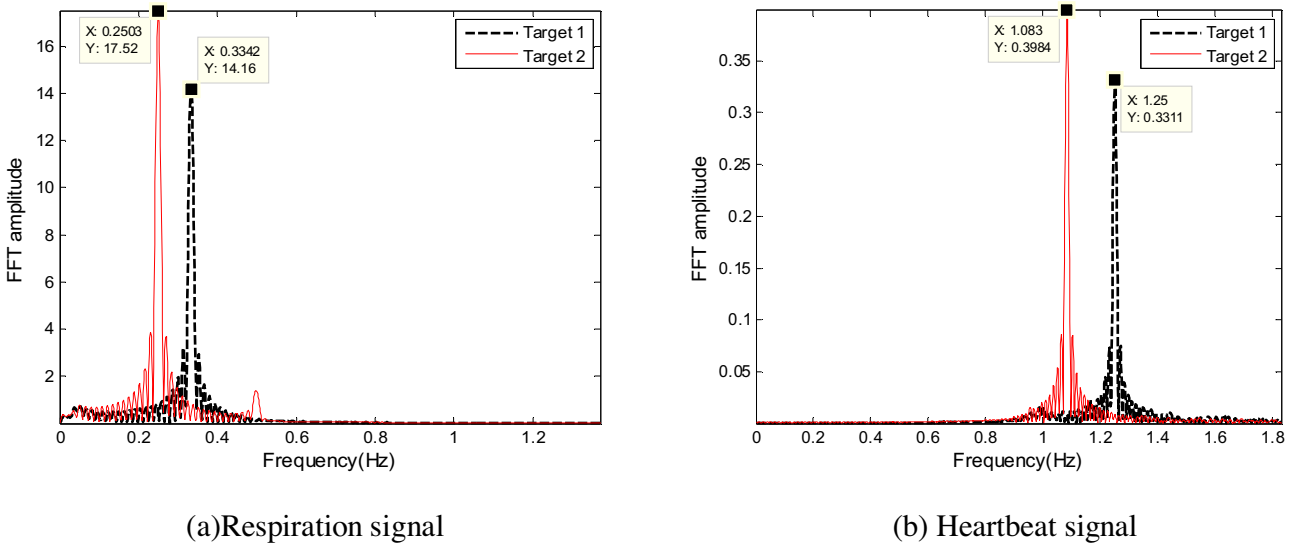

(a)Respiration signal (b) Heartbeat signal

Fig. 8. Frequency spectrums of extracted respiration and heartbeat signals of two targets by our method.

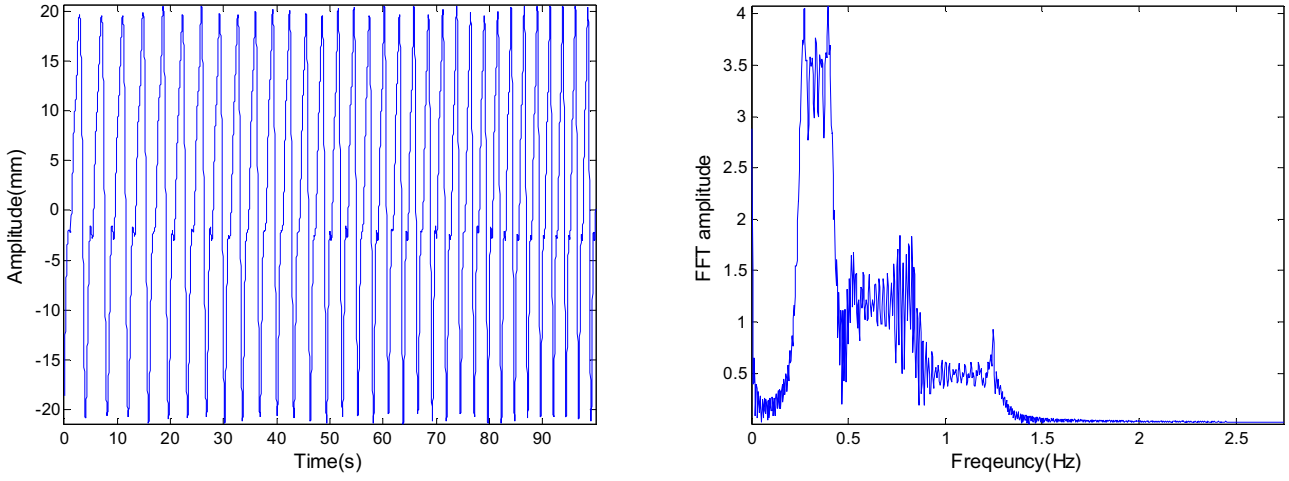

(a) Time domain (b) Frequency domain

Fig. 9. Physiological signal (i.e., heartbeat signal mixed with respiration signal with harmonics) and its frequency spectrum when the fundamental respiration rate varies from 14 bpm to 20 bpm over 100 s (heart rate is 75 bpm).

where $\hat{f}_p$ and f_p are the estimated frequency value and theoretical frequency value of the heartbeat or respiration signals respectively, when P different frequencies are calculated.

From Fig. 12, the frequency estimation for the heartbeat signal has a larger error when SNR is lower than around −12.2 dB and a smaller error when SNR is higher than −12 dB compared with the respiration signal.

4. Discussion

The FMCW wide-band radar can provide noncontact, continuous and timely cardiopulmonary monitoring for multiple human targets, which is convenient for patients and nurses. In addition, this radar system has the potential to have a compact size and a low power budget with no threat to human safety. These advantages enable the FMCW wide-band radar to be widely applied for monitoring in both hospitals and home healthcare or psychology studies.

In this paper, only the phase of the Fourier transform is used for demodulation of the displacement of targets. However, both the amplitude and phase of the Fourier transform were thought to contain information about the target movement in [16]. From the formula of the Fourier transform result (seen in Eq. (3)) of the FMCW radar in this paper, only the phase of the Fourier transform comprises the vibration information from targets. From Fig. 3, the amplitudes of clutter and targets do not vary over time, indicating that the amplitude of the Fourier transform does not contain vibration information from the targets.

The estimation precise of frequencies of vital signs is acceptable even when the SNR of the radar receiver is low by robustness analysis against noise seen from Fig. 12. Compared with the single frequency CW radar, the SNR of the demodulated phase of the FMCW radar is significantly improved by a Fourier transform in fast time. Because for the FMCW radar, the phase information from one range bin corresponding to a frequency point is accumulated after the Fourier transform of the beat signal. However, noise cannot be accumulated by the Fourier transform. Note that

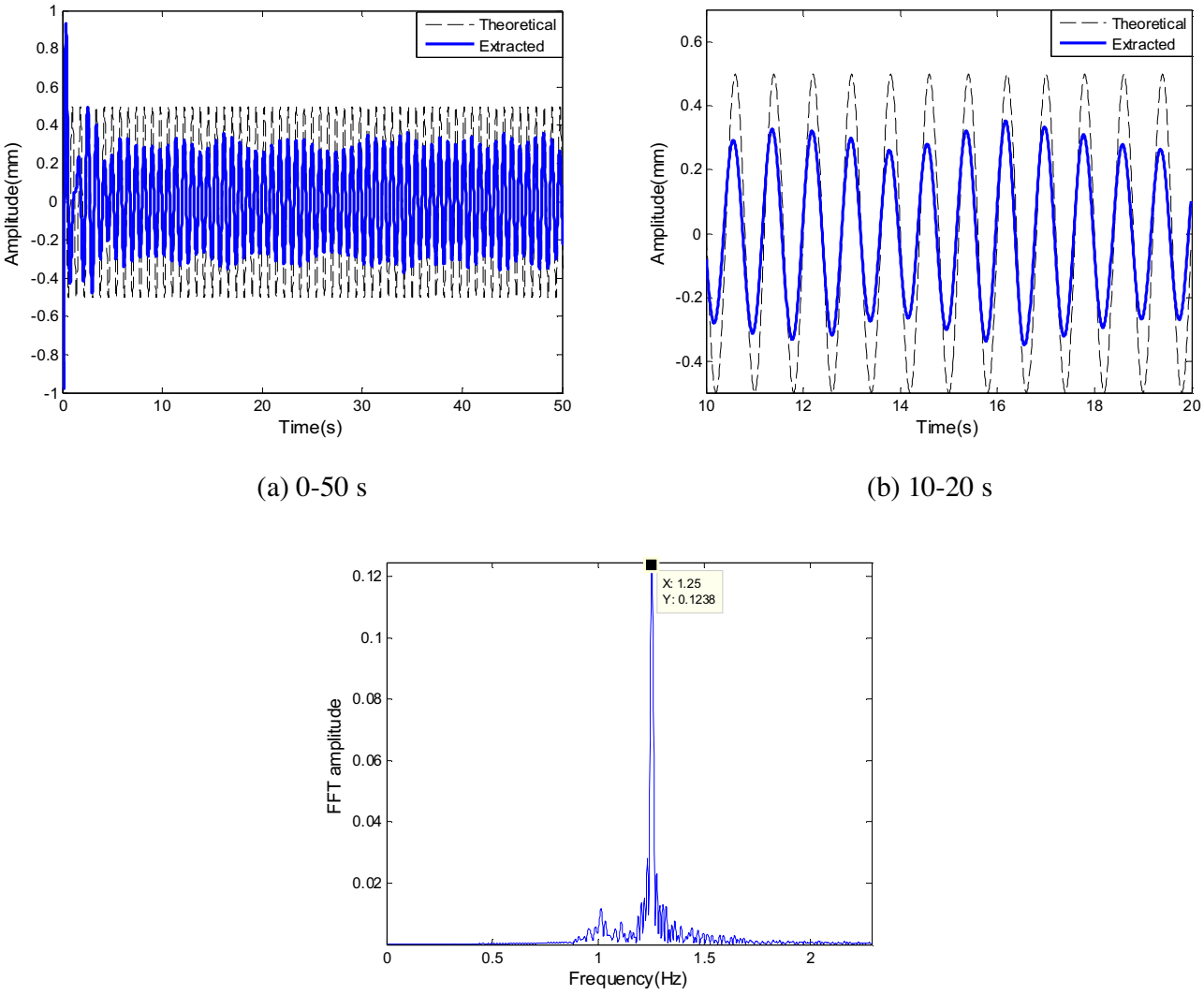

Fig. 10. When the respiration rate varies from 14 bpm to 20 bpm over 100 s, the extracted heartbeat signal compared with the theoretical heartbeat signal in the time domain (a) from 0 s to 50 s and (b) from 10 s to 20 s; (c) the frequency spectrum of the extracted heartbeat signal (heart rate is 75 bpm).

the accumulation and acquirement of phase information rely on the coherence maintenance for the radar, which can be assured by using some existing technologies, such as available direct digital synthesis, voltage-controlled oscillator and clock synchronization [18]. Assuming that the noise in the radar receiver is Gaussian white noise, the theoretical SNR improvement factor for the demodulated phase is $20 \times \log_{10}(N)$ dB. Thus, indoor monitoring did not require a high SNR for FMCW radar systems compared with single frequency CW radars. The SNR is normally improved by the accumulation of energy over a period of time for UWB radars. However, it is very difficult to monitor vital signs, especially heartbeat signals, with an extremely low SNR [31]. From Figs. 4 and 5, the absolute motion of the chest wall is precisely obtained under a low SNR for the FMCW radar.

This paper introduces a new separation method for respiration and heartbeat signals based on the double parameter LMS filter. No additional reference signal is needed in this filtering because the instantaneous respiration signal can be approximately acquired from the mixed physiological signal by moving average filtering and peak detection. Compared with the BPF method and the WT method, the proposed method can obtain more accurate respiration and heartbeat signals. In addition, our proposed method can separate respiration and heartbeat signals in real time with LMS filtering. In terms of complexity, for each sample of an input signal, the proposed algorithm requires $(4M+8)$ additions and $(6M+8)$ multiplications, where M represents the number of respiration harmonics. The varying frequency of the respiration signal, which usually happens in real-life situations, will not decrease the quality of the extracted heartbeat signal, especially the heart rate. Otherwise, the projection matrix method that needs to implement the eigenvalue decomposition of the large size correlation matrix [23] and the continuous-wavelet filter and EEMD based algorithm [4] are time consuming and result in a heavy burden to the digital signal processing module of the radar system. In the EEMD-based algorithm, the varying frequency of the respiration signal will disturb the choice of certain intrinsic mode functions to reconstruct the heartbeat signal [4].

In our proposed method, the choice of a proper value for the initial step size μ_0 is very important. When μ_0 is smaller than 0.54, the larger the value is, and the faster the extracted signal convergence rate. However, large μ_0 will decrease the amplitude of an extracted heartbeat signal according to $\frac{\mu_0 f_s}{M\pi}$, especially when

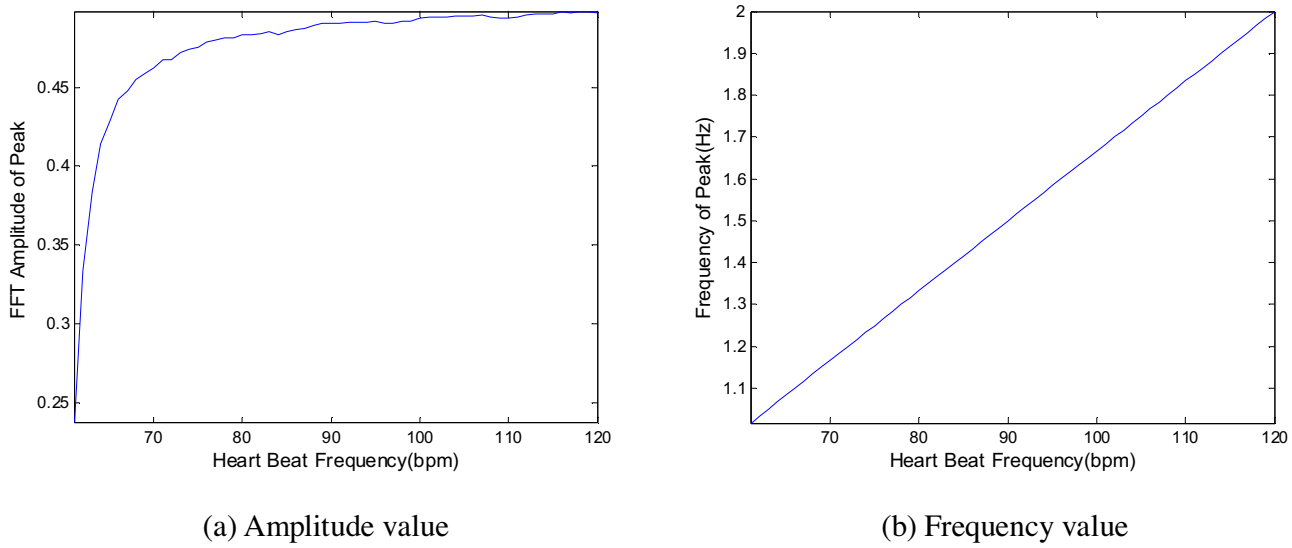

Fig. 11. The amplitude (a) and frequency (b) values of the peaks on the frequency spectrums of the extracted heartbeat signals change with heart rate variation from 61 bpm to 80 bpm with a step of 1 bpm when the fundamental respiration rate is 20 bpm with two harmonics.

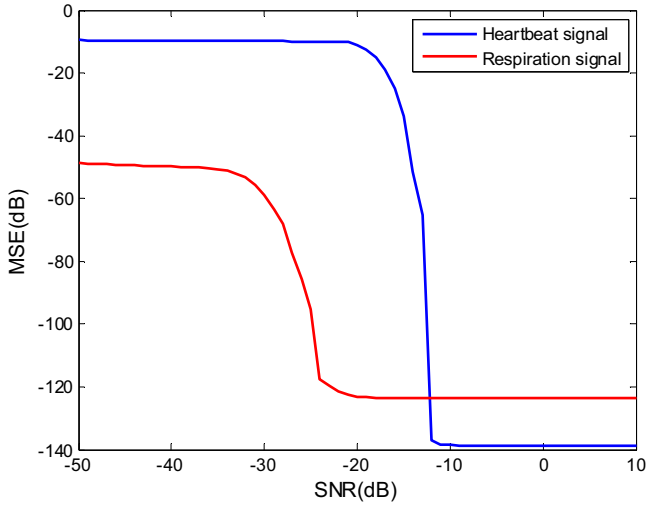

Fig. 12. The MSEs are plotted as functions of SNR for the heartbeat and respiration signals.

the frequency of a high order harmonic of the respiration signal is close to the frequency of the heartbeat signal. For a compromise, we chose μ_0 to be 0.005. The convergence time is approximately 1 s for the extracted respiration signal and is shorter than 20 s for the extracted heartbeat signal even when the respiration signal frequency varies, which is acceptable for long-term monitoring. Details of the choice of the initial step size μ_0 value are not presented in this paper because the aim of the paper is not to validate an optimum μ_0 value, but rather to demonstrate the efficiency of the proposed method. Additionally, another parameter participating in decreased amplitude of the extracted heartbeat signal is the sampling frequency of the physiological signal. Considering a smaller reduction in amplitude, we decimate the sampling rate of the radar signal in slow time from the default value PFR to 100 Hz; this value is high enough for the chest wall movement.

Detection of multiple subjects has been reported in only a few studies [14,24,32,33]. CW Doppler radars were used to distinguish at most two subjects, but it cannot distinguish heart rates of individual subjects [32]. A UWB radar, consisting of one transmitting antenna and three receiving antennas, was developed to determine target count based on correlation processing of sensed respiration among the data channels [33]. However, estimation of the physiological signals and localization of multiple targets was not realized. In [14], a logarithmic method was proposed to utilize the phase information to accurately detect the heart rates in two subjects. A hybrid FMCW-interferometry radar was proposed to track the location of individuals and monitor their life activities [24]. However, multiple subject detection was realized by 2-D scanning both in [24] and [14]. This paper provides a framework of multi-target monitoring using the FMCW wide-band radar. Not only the range or position of multi-targets can be obtained but also their correlation with respiration and heartbeat signals can be obtained without scanning. In addition, the framework also offers a solution for clutter suppression.

The limitation of this study is that only the simulation data are used to verify the proposed framework and algorithm; cases of large body motion across range bins are not considered in the simulation. However, simulations have the advantage of demonstrating some theoretical deductions and facts that may be disturbed and confused when only the measurement data are adopted because the measurement data may be contaminated by unexpected clutter or the non-ideality of the system. In our future work, the FMCW wideband radar will be developed to evaluate multi-human target monitoring in wards or at home.

5. Conclusion

The FMCW wide-band radar is a reliable, robust, and harmless tool for real-time monitoring of multiple cardiac and respiratory rates and subject localization. The absolute chest wall motion is precisely obtained under a low SNR for the FMCW radar. Compared with the BPF method and the WT method, the proposed method based on a double parameter LMS filter can obtain more accurate respiration and heartbeat signals, especially when the respiration signal has multiple harmonics and varying frequencies. No additional reference signal is needed in the proposed method. With a proper initial step size, the respiration and heartbeat signals can quickly converge and maintain a smaller steady-state offset the next time. An FMCW wideband radar system will be developed to launch the experiment of multi-human target monitoring in wards or at home in our future work.

Acknowledgment

This work was supported by the National Natural Science Foundation of China (nos.41301397).

References

[1] K. van Loon, M. Breteler, L. van Wolfwinkel, A. Rheineck Leyssius, S. Kossen, C. Kalkman, B. van Zaane, L. Peelen, Wireless non-invasive continuous respiratory monitoring with FMCW radar: a clinical validation study, J. Clin. Monit. Comput. (2015) 1–9.
[2] W. Massagram, V.M. Lubecke, A. Høst-Madsen, O. Boric-Lubecke, Assessment of heart rate variability and respiratory sinus arrhythmia via Doppler radar, IEEE Trans. Microw. Theory Tech. 57 (2009) 2542–2549.
[3] C. Li, J. Cummings, J. Lam, E. Graves, W. Wu, Radar remote monitoring of vital signs, IEEE Microw. Mag. 10 (2009) 47–56.
[4] W. Hu, Z. Zhao, Y. Wang, H. Zhang, F. Lin, Noncontact accurate measurement of cardiopulmonary activity using a compact quadrature doppler radar sensor, IEEE Trans. Biomed. Eng. 61 (2014) 725–735.
[5] Y. Xiao, J. Lin, O. Boric-Lubecke, V.M. Lubecke, Frequency-tuning technique for remote detection of heartbeat and respiration using low-power double-sideband transmission in the Ka-band, IEEE Trans. Microw. Theory Tech. 54 (2006) 2023–2032.
[6] J.E. Kiriazi, O. Boric-Lubecke, V.M. Lubecke, Dual-frequency technique for assessment of cardiopulmonary effective RCS and displacement, IEEE Sens. J. 12 (2012) 574–582.
[7] C. Li, Y. Xiao, J. Lin, Experiment and spectral analysis of a low-power Ka-band heartbeat detector measuring from four sides of a human body, IEEE Trans. Microw. Theory Tech. 54 (2006) 4464–4471.
[8] T.J. Kao, Y. Yan, T. Shen, A.Y. Chen, J. Lin, Design and analysis of a 60-GHz CMOS doppler, IEEE Trans. Microw. Theory Tech. 61 (2013) 1649–1659.
[9] B.K. Park, V.M. Lubecke, O. Boric-Lubecke, Arctangent demodulation with DC offset compensation in quadrature Doppler radar receiver systems, IEEE Trans. Microw. Theory Tech. 55 (2007) 1073–1079.
[10] C. In, L. Dong-Woo, K. Jae-Mo, L. Jae-Hwan, K. Hyung-Myung, K. Seongdo, C. Kim, Human detection based on the condition number in the non-stationary clutter environment using UWB impulse radar, in: 2013 Asia-Pacific Microwave Conference Proceedings (APMC), Piscataway: IEEE Press, Seoul, 2013, pp. 1006–1008.
[11] Z. Li, W. Li, H. Lv, Y. Zhang, X. Jing, J. Wang, A novel method for respiration-like clutter cancellation in life detection by dual-frequency IR-UWB radar, IEEE Trans. Microw. Theory Tech. 61 (2013) 2086–2092.
[12] B. Schleicher, I. Nasr, A. Trasser, H. Schumacher, IR-UWB radar demonstrator for ultra-fine movement detection and vital-sign monitoring, IEEE Trans. Microw. Theory Tech. 61 (2013) 2076–2085.
[13] N. Van, A.Q. Javaid, M.A. Weitnauer, Harmonic path (HAPA) algorithm for non-contact vital signs monitoring with IR-UWB radar, in: Biomedical Circuits and Systems Conference (BioCAS) Rotterdam, Piscataway:IEEE Press, the Netherlands, 2013, pp. 146–149.
[14] L. Ren, Y.S. Koo, H. Wang, Y. Wang, Q. Liu, A.E. Fathy, Noncontact multiple heartbeats detection and subject localization using UWB impulse Doppler radar, IEEE Microw. Wireless Compon. Lett. 25 (2015) 690–692.
[15] J.C.Y. Lai, Y. Xu, E. Gunawan, E.C. Chua, A. Maskooki, Y.L. Guan, K.S. Low, C.B. Soh, C.L. Poh, Wireless sensing of human respiratory parameters by low-power ultrawideband impulse radio radar, IEEE Trans. Instrum. Meas. 60 (2011) 928–938.
[16] L. Anitori, A. de Jong, F. Nennie, FMCW radar for life-sign detection, in: Radar Conference, 2009 IEEE, Pasadena, CA, 2009, pp. 1–6.
[17] K. Mostov, E. Liptsen, R. Boutchkoa, Medical applications of shortwave FM radar: remote monitoring of cardiac and respiratory motion, Am. Assoc. Phys. Med. 37 (2010) 1332–1338.
[18] G. Wang, J.M. Muñoz-Ferreras, C. Gu, C. Li, R. Gómez-García, Application of linear-frequency-modulated continuous-wave (LFMCW) radars for tracking of vital signs, IEEE Trans. Microw. Theory Tech. 62 (2014) 1387–1399.
[19] J.M. Muñoz-Ferreras, G. Wang, C. Li, R. Gómez-García, Mitigation of stationary clutter in vital-sign-monitoring LFMCW radars, IET Radar Sonar Navig. 9 (2015) 138–144.
[20] C. Li, V.M. Lubecke, O. Boric-Lubecke, J. Lin, A review on recent advances in Doppler radar sensors for noncontact healthcare monitoring, IEEE Trans. Microw. Theory Tech. 61 (2013) 2046–2060.
[21] E. Pasqua, UWB FMCW Radar for Concealed Weapon Detection: RF Front-end Development, Delft University of Technology, Delft, Netherlands, 2012, vol. Master.
[22] Ø. Aardal, Y. Paichard, S. Brovoll, T. Berger, T.S. Lande, S. Hamran, Physical working principles of medical radar, IEEE Trans. Biomed. Eng. 60 (2013) 1142–1149.
[23] D. Zhang, M. Kurata, T. Inaba, FMCW radar for small displacement detection of vital signal using projection matrix method, Int. J. Antennas Propag. 2013 (2013) 1–5.
[24] G. Wang, C. Gu, T. Inoue, C. Li, A hybrid FMCW-interferometry radar for indoor precise positioning and versatile life activity monitoring, IEEE Trans. Microw. Theory Tech. 62 (2014) 2812–2822.
[25] D.R. Morgan, M.G. Zierdt, Novel signal processing techniques for Doppler radar cardiopulmonary sensing, Signal Process. 89 (2009) 45–66.
[26] M. He, Y. Nian, B. Liu, Noncontact heart beat signal extraction based on wavelet transform, in: International Conference on BioMedical Engineering and Informatics, Shengyang, 2015, pp. 209–213.
[27] M.A. Colominas, G. Schlotthauer, M.E. Torres, Improved complete ensemble EMD: a suitable tool for biomedicalsignal processing, Biomed. Signal Process. Control 14 (2014) 19–29.
[28] M. He, Y. Nian, X. Wang, S. Xiao, Y. Li, Improved clutter suppression algorithm for atmospheric target detection using polarimetric doppler radar, IEEE J. Sel. Top. Appl. Earth Obs. Remote Sens. 4 (2011) 911–922.
[29] C. Oliver, S. Quegan, Understanding Synthetic Aperture Radar Images, SciTech Publishing, Raleigh, 2004.
[30] Y. Xiao, Y. Tadokoro, LMS-based notch filter for the estimation of sinusoidal signals in noise, Signal Process. 46 (1995) 223–231.
[31] W.Z. Li, Z. Li, H. Lv, G.H. Lu, Y. Zhang, X.J. Jing, S. Li, J.Q. Wang, A new method for non-line-of-sight vital sign monitoring based on developed adaptive line enhancer using low centre frequency UWB radar, Progr. Electromag. Res. 133 (2013) 535–554.
[32] Q. Zhou, J. Liu, A. Host-Madsen, O. Boric-Lubecke, V. Lubecke, Detection of multiple heartbeats using Doppler radar, in: Proc. IEEE ICASSP, Toulouse, 2006, pp. 1160–1163.
[33] H. Lv, M. Liu, J. Teng, Z. Yang, Y. Xiao, S. Li, X. Jing, J. Wang, Multi-target human sensing via UWB bio-radar based on multiple antennas, in: 2013 IEEE International Conference of IEEE Region 10 (TENCON 2013), Piscataway: IEEE Press, Xi'an, China, 2013, pp. 1–4.